# Low doses of ultraviolet radiation and oxidative damage induce dramatic accumulation of mitochondrial DNA replication intermediates, fork regression, and replication initiation shift

Rubén Torregrosa-Muñumer, Steffi Goffart, Juha A. Haikonen, and Jaakko L.O. Pohjoismäki
Department of Biology, University of Eastern Finland, 80101 Joensuu, Finland

**ABSTRACT** **Mitochondrial DNA is prone to damage by various intrinsic as well as environmental stressors. DNA damage can in turn cause problems for replication, resulting in replication stalling and double-strand breaks, which are suspected to be the leading cause of pathological mtDNA rearrangements. In this study, we exposed cells to subtle levels of oxidative stress or UV radiation and followed their effects on mtDNA maintenance. Although the damage did not influence mtDNA copy number, we detected a massive accumulation of RNA:DNA hybrid–containing replication intermediates, followed by an increase in cruciform DNA molecules, as well as in bidirectional replication initiation outside of the main replication origin, $O_H$. Our results suggest that mitochondria maintain two different types of replication as an adaptation to different cellular environments; the RNA:DNA hybrid–involving replication mode maintains mtDNA integrity in tissues with low oxidative stress, and the potentially more error tolerant conventional strand-coupled replication operates when stress is high.**

**Monitoring Editor**
Thomas D. Fox
Cornell University

Received: Jun 15, 2015
Revised: Sep 10, 2015
Accepted: Sep 14, 2015

## INTRODUCTION

Mitochondria are cell organelles responsible for oxygen-dependent production of ATP, which can be used as energy currency in many cellular processes. Mitochondria have their own genome, mitochondrial DNA (mtDNA), which in mammals is typically a 16.5-kb circular double-stranded molecule existing in thousands of copies per cell. mtDNA encodes for 13 subunits of protein complexes involved in oxidative phosphorylation (OXPHOS), as well as for tRNAs and rRNAs required for their translation, and is therefore essential for mitochondrial ATP production and other mitochondrial functions.

Because mtDNA is located in close vicinity to the electron transport chain, mitochondrial DNA is expected to be especially prone to oxidative damage caused by reactive oxygen species (ROS; Lagouge and Larsson, 2013). Oxidative damage can cause the formation of 5,6-dihydroxy-5,6-dihydrothymidine (thymidine glycol [Tg]) and 8-oxo-7-hydrodeoxyguanosine (8-oxodG) in DNA (Frenkel *et al.*, 1981; Floyd *et al.*, 1986). Whereas Tg can block DNA synthesis (Aller *et al.*, 2007), 8-oxodG frequently mispairs with A, resulting in G>T (or C>A) transversions (Cheng *et al.*, 1992). Of interest, mtDNA mutations observed in aged organisms do not show any G>T bias, and the bulk of mutation load instead seems to result from random replication errors obtained over time (Lagouge and Larsson, 2013). However, if oxidative stress is intensive, such as in heart of heterozygous mitochondrial superoxide dismutase (SOD2)–knockout mice, a clear increase in G>T transversions can be observed (Pohjoismaki *et al.*, 2013). Together with the elevated mutation load, the *Sod2*$^{+/-}$ mouse hearts show also high levels of mtDNA rearrangements and replication stalling.

This article was published online ahead of print in MBoC in Press (http://www.molbiolcell.org/cgi/doi/10.1091/mbc.E15-06-0390) on September 23, 2015.

The authors declare that they have no conflicts of interest with regard to the contents of this article.

Address correspondence to: Jaakko L. O. Pohjoismäki (Jaakko.Pohjoismaki@uef.fi).

Abbreviations used: 2D-AGE, two-dimensional agarose gel electrophoresis; 8-oxodG, 8-oxo-7-hydrodeoxyguanosine; BER, base excision repair; COSCOFA, conventional strand-coupled Okazaki-fragment–associating (mtDNA replication mode with dsDNA intermediates); ddC, 2,3 dideoxycytidine; dsDNA, double-stranded DNA; mtDNA, mitochondrial DNA; nDNA, nuclear DNA; NER, nucleotide excision repair; OXPHOS, oxidative phosphorylation; RITOLS, RNA intermediates throughout the lagging strand (RNA intermediate–containing, strand-asymmetric mtDNA replication mode); ROS, reactive oxygen species; Td or T=T, cyclobutane pyrimidine dimers, thymidine dimers; Tg, 5,6-dihydroxy-5,6-dihydrothymidine or thymidine glycol.

Besides oxidative damage, ultraviolet (UV) radiation–induced cyclobutane pyrimidine dimers (including thymidine dimers [Td or T=T]) and 6-4 photoproducts can also block replication fork progression (McCulloch *et al.*, 2004). Whereas oxidized nucleotides can be efficiently removed by mitochondrial base excision repair (BER), UV damage causes bulky lesions, which distort the helix and need to be repaired by nucleotide excision repair (NER). Although evidence exists that certain members of the nuclear NER machinery might localize to mitochondria of cardiomyocytes (Pohjoismaki *et al.*, 2012), NER activity has not been found in mitochondria (Gredilla *et al.*, 2010).

Although mitochondrial DNA replication stress has been implicated to be the leading cause of pathological mtDNA rearrangements (Krishnan *et al.*, 2008), nothing is known of replication fork stalling and processing in mitochondria. For example, in bacteria, DNA damage stalls the leading-strand polymerase but does not impair lagging-strand synthesis (Yeeles and Marians, 2011). This has potentially interesting consequences for mitochondria, as the main mode of mtDNA replication is highly strand asymmetric, and the lagging-strand DNA is synthesized with considerable delay in most tissues (Pohjoismaki *et al.*, 2011). The lagging-strand template is originally covered by preformed RNA, resulting in specific RNaseH-sensitive replication intermediates (i.e., RNA intermediates throughout the lagging strand [RITOLS]; Reyes *et al.*, 2013). However, a strand-coupled mechanism characterized by fully double-stranded DNA (dsDNA) replication intermediates (i.e., conventional strand-coupled Okazaki-fragment associating [COSCOFA]) coexists with the strand-asymmetric mechanism in all tissues and is in fact the dominant replication mode in tissues such as skeletal muscle, heart, and brain (Goffart *et al.*, 2009; Pohjoismaki *et al.*, 2009). Whereas the strand-asymmetric mechanism initiates at $O_H$ (Holt and Reyes, 2012), little is known about the initiation of strand-coupled replication. As the bidirectionally progressing replication bubbles outside of the noncoding region of mtDNA are fully dsDNA, it is likely that strand-coupled replication initiates mainly from a wider region of mtDNA, known as Ori-Z (Bowmaker *et al.*, 2003; Pohjoismaki and Goffart, 2011). Note that Ori-Z is not a defined location, but that replication initiation can likely occur at multiple origins in a region spanning approximately the nucleotides 10,500–16,000 of human mtDNA. Nothing is known about the licensing of these origins, and the evidence of their existence is based on two-dimensional agarose gel electrophoresis (2D-AGE; Bowmaker *et al.*, 2003), as well as on transmission electron microscopy (Pohjoismaki *et al.*, 2011).

The aim of our study was to investigate the responses that different types of DNA damage cause with regard to mtDNA maintenance. To do this, we exposed HEK293 cells to oxidative and UV damage and followed the fate of mitochondrial replication intermediates. of interest, the two damage types caused almost identical replication-stalling phenotypes in cells, with a long-lasting increase in RNA-containing intermediates, followed by an increase in strand-coupled replication initiation outside $O_H$. Despite the striking mtDNA replication phenotype, we did not observe any effect on mtDNA copy number. We propose that mitochondria maintain two different replication mechanisms, of which the strand-asynchronous mechanism could represent a high-fidelity mode, whereas the strand-coupled replication is a more-damage-tolerant mode, operating under genotoxic stress and potentially explaining its preference in highly oxidative tissues.

## RESULTS

### The effects of oxidative and UV damage on mtDNA

Oxidative stress in mitochondria will also impose oxidative stress on the nucleus (Kaniak-Golik and Skoneczna, 2015), and therefore the two effects cannot be completely disconnected in any experimental modeling. Mitochondrial ROS can be specifically induced by electron transport chain inhibitors, but these drugs cause detrimental effects on cells while producing only low levels of ROS in cultured cells such as HEK293 (Han and Im, 2008). The more general oxidizing agent $H_2O_2$ can generate biologically significant ROS, namely the reactive hydroxyl radical (OH·), through the $Fe^{2+}$-catalyzed Fenton reaction. Although $H_2O_2$ has been widely used as ROS source in experiments, it has a short half-life in cells, making the use of non-toxic chronic exposure levels difficult to control (Wagner *et al.*, 2013). We therefore decided to use a less known agent, $KBrO_3$, which is capable of specifically inducing oxidative DNA damage (Ballmaier and Epe, 1995) at a relatively low concentration of 30 μM to avoid off-target effects in the cells (Kawanishi and Murata, 2006). As far as is known and similarly to $H_2O_2$, $KBrO_3$ is not specific to mtDNA but will equally damage nuclear DNA (nDNA). To control this, we estimated the effect on cell survival and nDNA damage signaling under the influence of $KBrO_3$ (Supplemental Figures S1 and S2). Although no effect on cell survival was observed, $KBrO_3$ induced a transient increase in the nuclear DNA damage marker H2A.X phosphorylation at Ser-139 (Supplemental Figure S2A). Note that the increase in H2A.X phosphorylation was more extreme after UV damage and persisted for up to 64 h after exposure (Supplemental Figure S2B). Both UV and $H_2O_2$ induced a significant and persistent activation of the checkpoint kinase Chk1, whereas $KBrO_3$ had only a very mild and transient effect on this nuclear damage marker (Supplemental Figure S2, A–C; see the Supplemental Material for further details).

Although $KBrO_3$ did not have as dramatic an effect on nuclear DNA damage signaling as UV or $H_2O_2$, it induced a marked increase in mtDNA damage (Figure 1A). The damage did not result in copy number depletion or any effect on the supercoiling of mtDNA (Figure 1, C and D). Of interest, the treatment with $H_2O_2$ induced an increase in mtDNA levels (Supplemental Figure S2D). Because $H_2O_2$ is also a known activator of mitochondrial biogenesis (Spiegelman, 2007), this could indicate that this effect is not a reaction to mtDNA damage but instead is caused via nuclear gene regulation.

Next we wanted to compare these effects with a mild UV treatment of 1.34 mJ/cm$^2$ s for 30 s on the cells. At this dosage, UV did not have any effect on cell survival or proliferation (Supplemental Figure S1). Because mitochondria are not expected to have nucleotide excision repair (Liu and Demple, 2010)—the main mechanism to repair UV-induced photoproduct lesions—the effect on mtDNA should be markedly greater than on nDNA. Although we were able to detect mtDNA damage after UV exposure, this treatment also did not significantly affect mtDNA copy number or topology (Figure 2). The UV treatment differed from the $KBrO_3$ experiment, as the exposure to the damaging agent was brief and only the recovery could be followed, not any chronic exposure effects.

In contrast to UV and $KBrO_3$ treatments, the specific inhibitor of mtDNA replication 2,3-dideoxycytidine (ddC) had a rapid and profound effect on mtDNA copy number without any effects on nDNA damage signaling (Supplemental Figure S3).

### UV and $KBrO_3$ induce a specific accumulation of mtDNA replication intermediates

To see how the different damage agents influence mtDNA replication, we used 2D-AGE concentrating on the *Hin*cII restriction fragment containing the entire noncoding region (NCR) with the main mitochondrial replication origin $O_H$. Replication stalling in this region can be typically seen especially as an increase in the replication bubble structures (Wanrooij *et al.*, 2007). Both UV and $KBrO_3$

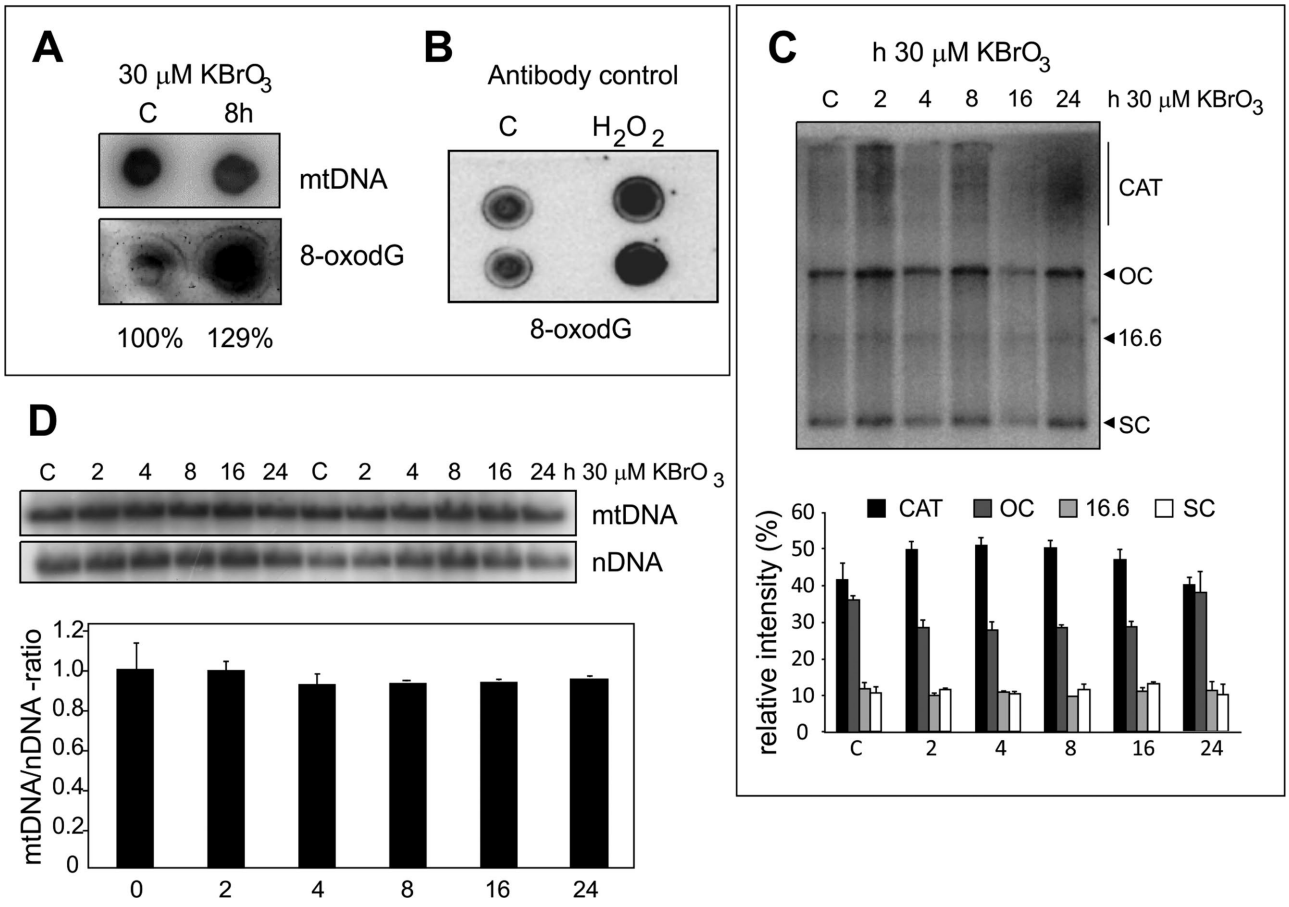


FIGURE 1: Effects of $KBrO_3$ on mtDNA copy number and topology. (A) Dot-blot of purified mtDNA from control cells and cells treated with 30 μM $KBrO_3$. Oxidative damage is detected using an antibody against 8-oxodG by South-Western analysis and normalized against total mtDNA by Southern hybridization on a separate blot. (B) Dot-blot for antibody verification, showing control mtDNA and mtDNA treated in vitro with 7.4% $H_2O_2$ for 30 min. (C) Topology gel of mtDNA. $KBrO_3$ treatment had no effect on mtDNA topology.16.6, 16.6-kb linear molecules; CAT, catenanes; OC, open circles; SC, supercoiled mtDNA. (D) mtDNA copy number levels during the $KBrO_3$ treatment time course. Despite the damage, mtDNA copy number is not affected by $KBrO_3$.

treatment increased the relative amount of NCR replication bubbles (Figure 3). However, unlike in the case of replication stalling caused by ddC, where a distinct sharp dsDNA bubble arc of COSCOFA type is detected, the intermediates in UV and $KBrO_3$ treatments were diffuse, RNA-containing RITOLS replication bubbles (Yasukawa *et al.*, 2006; Wanrooij *et al.*, 2007).

To investigate whether the treatments specifically influence the RNA-containing intermediates, we also studied restriction fragments producing prominent slow-moving RITOLS arcs, such as the *Dra*I fragment spanning nucleotides 12,273–16,012. Indeed, a strong and specific increase in the RITOLS arc was detected in the UV- and $KBrO_3$-treated cells (smy in Figure 4). In contrast, ddC treatment leads to a strong increase in dsDNA COSCOFA replication intermediates but not smy in this fragment. Of interest, in $H_2O_2$-treated cells, no major effect on mtDNA replication intermediates could be observed (Supplemental Figure S2D).

We next sought to see how mitochondrial DNA recovers from the damage and what happens to the accumulated replication intermediates during the recovery process. Because we did not detect any deleterious influence on cell survival, and knowing that DNA repair processes in the nucleus are fast (Peterson and Almouzni, 2013), we assumed that also the processing of damaged mtDNA would occur in a matter of hours. To our surprise, the abnormal RITOLS arc persisted for up to 64 h (Figure 5 and Supplemental Figure S4). During the recovery process, an increase in cruciform molecules (x and xr in Figure 5), as well as in replication bubbles outside the NCR, was detected. Of interest, despite the initial differences in stalling phenotype, the recovery from ddC exposure also resulted in a greater abundance of RITOLS (Figure 6).

### UV and $KBrO_3$ treatments increase the steady-state levels of mitochondrial mRNAs

To understand why there is such a persistent change in the RNA-containing mtDNA replication intermediates, we analyzed the levels of some mitochondrial mRNAs, including ND3 mRNA, which was previously shown to be a sensitive marker for changes in mitochondrial transcription (Pohjoismaki *et al.*, 2006). Of interest, both UV and $KBrO_3$ treatment induced a delayed, long- term increase in ND2 levels but dissimilar effects on ND3 (Figure 7, A and B). In addition, the levels of polycistronic transcript from which the mRNAs are generated were strongly depleted by the UV treatment. In agreement with the loss of the primary transcripts, the UV-treated cells also showed a reduction in the mitochondrial transcription rate (Figure 7C).

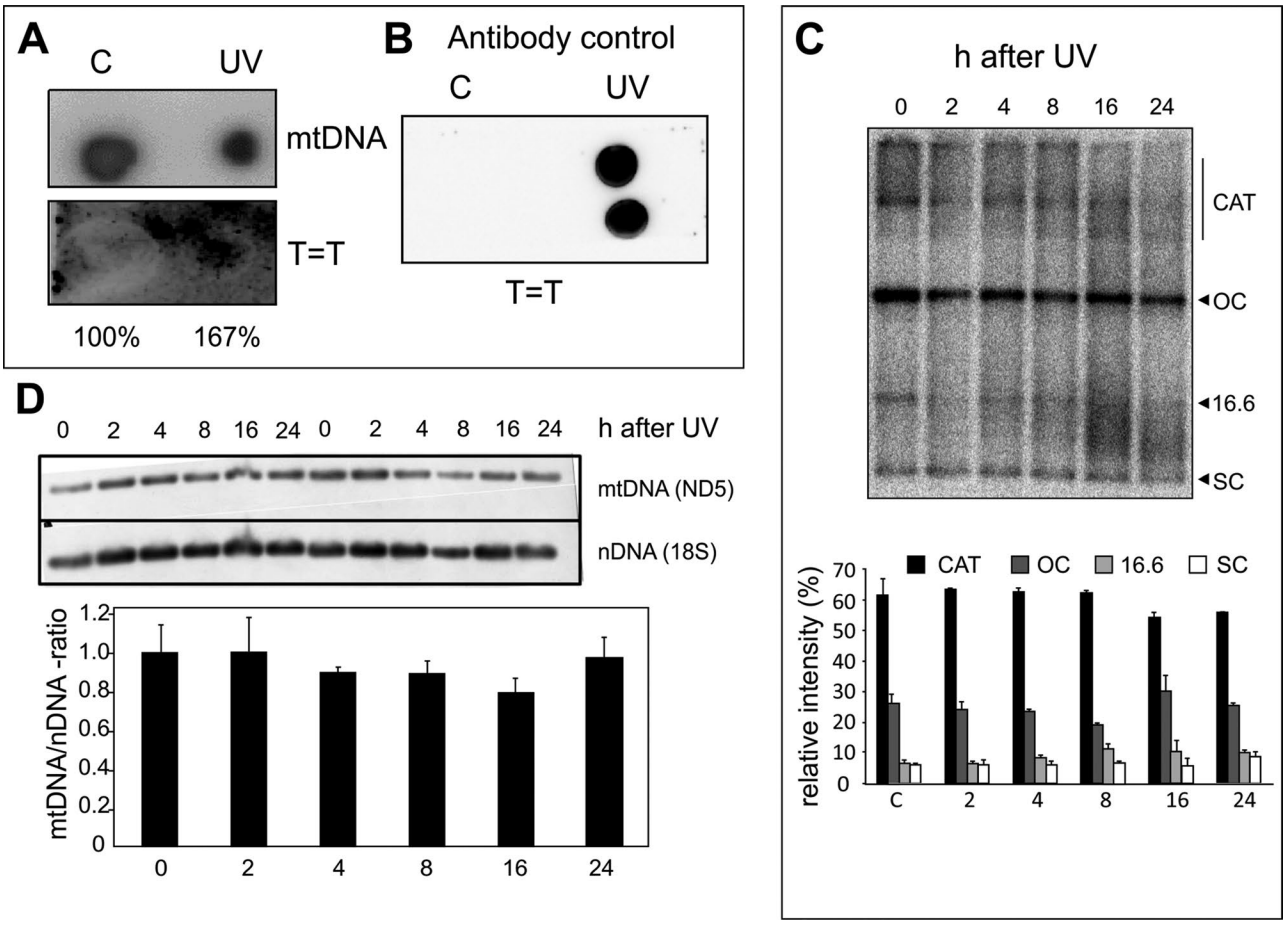


FIGURE 2: UV treatment has no major effect on mtDNA copy number and topology. (A) A dot-blot of purified mtDNA from control and HEK cells treated with 1.34 mJ/cm$^2$ s UVB (305 nm) for 30 s. Thymidine dimers (T=T) are detected using a specific antibody and normalized against total mtDNA on a sister blot. (B) A dot-blot for antibody control, showing untreated mtDNA and mtDNA treated in vitro with 1.34 mJ/cm$^2$ s for 5 min. The detected signal is far stronger than in A, explaining the difference in the background noise. UV treatment did not significantly alter (C) topology or (D) mtDNA copy number.

## DISCUSSION

Mitochondrial DNA is prone to the same types of damage as nuclear DNA, and it is likely that mtDNA damage plays a role in many human diseases, as well as in normal ageing (Greaves *et al.*, 2012; Pinto and Moraes, 2014). However, the size of mtDNA compared with the nuclear genome quite likely makes a dramatic difference to the strategy how the two genomes cope with damage. Whereas the nuclear genome comprises billions of base pairs having only two copies of some essential genes, mtDNA is only 16.5 kb and exists in hundreds to thousands of copies per cell. In fact, it has been suggested that selective degradation or abandonment of mtDNA is much more cost efficient for the cell than its repair (Bendich, 2013). Although this might be the case to a certain extent, there can be instances in which mtDNA is under chronic genotoxic stress and finding intact copies for replication or transcription could become impossible without some adaptive mechanisms. In our approach, we sought to mimic such naturally occurring stress sources, such as the increased oxidative stress in metabolically active tissues, as well as exposure to sunlight's UV radiation, and see how the mitochondria cope with these types of insults.

Whereas UV and $KBrO_3$ treatments did not influence the host cell's survival (Supplemental Figure S1), we witnessed a dramatic effect on mtDNA replication intermediates (Figures 3 and 4). Unlike the POLG inhibitor ddC, which induces the stalling of all types of replication intermediates, UV and oxidative damage resulted in preferential increase in the RNA-containing RITOLS intermediates. Despite this apparent replication stalling, UV and oxidative damage did not induce a detectable change in mtDNA copy number (Figures 1 and 2). This observation could be explained by delayed maturation of such intermediates, without influencing the actual replication progression. However, this would be contrary to the situation in bacteria, in which DNA damage impairs specifically the leading-strand synthesis (Yeeles and Marians, 2011), whereas the RNA in RITOLS precedes the lagging-strand synthesis (Holt and Jacobs, 2014). A likely explanation is that the increase in RITOLS intermediates does not represent replication stalling per se but results from the increased recruitment of RNA into the replication fork. Of interest, UV treatment resulted in elevated levels of heavy-strand transcript ND2 (Figure 7A). Given that UV at the same time resulted in the loss of polycistronic primary transcripts, it is likely that the observed increase in the ND2 was not due to increase in transcription but instead to the stabilization of steady-state levels of the processed transcripts. This is also supported by the fact that ND3, although generated from the same primary transcript, did not show a similar increase as ND2. As a further demonstration, mitochondria from cells treated with UV showed impaired transcriptional activity

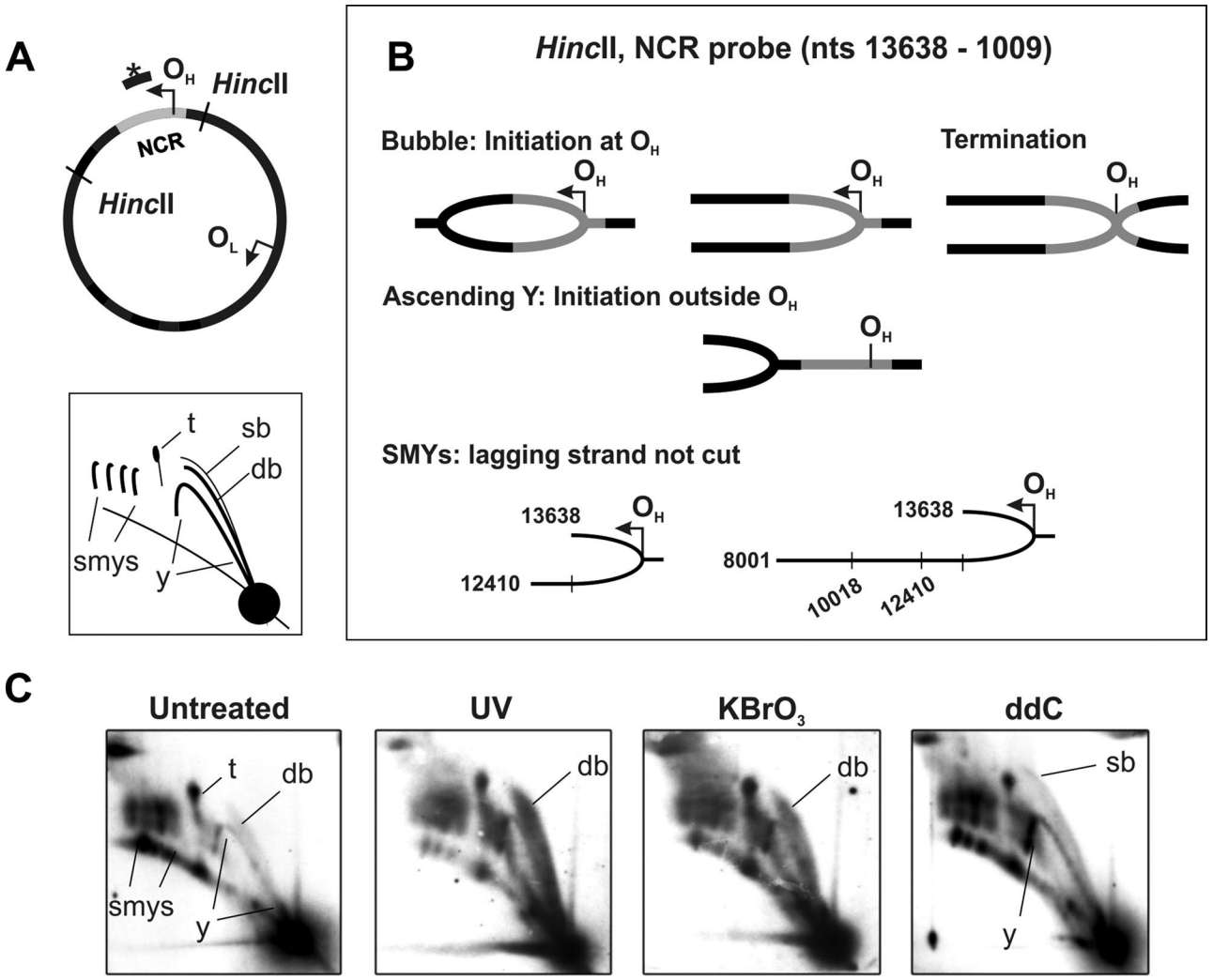


FIGURE 3: UV and $KBrO_3$ treatments increase the relative quantity of RNA:DNA hybrid replication bubbles in fragments containing the noncoding region of mtDNA. (A) Schematic presentation of the human mtDNA showing the NCR (gray), probe location (black bar with asterisk), replication origins ($O_H$, $O_L$), and the analyzed *Hin*cII 13,638–1009 fragment. (B) The different types of replication intermediates present in the analyzed region. Regular Y-arcs (y) represent simple replication forks; however, note that the full Y can be only obtained if there is replication initiation outside this region. Two types of replication bubbles are initiated at $O_H$: diffuse, RNA:DNA hybrid–containing (db) and sharp, dsDNA-containing forms (sb). The region around $O_H$ functions also as a replication terminus, where the replication forks from opposite directions meet and form an X-shaped molecule (t). Slow-moving Y-arcs (smys) are generated from RITOLS intermediates where the lagging strand is not cut by the restriction enzyme due to RNA:DNA hybrid at the restriction site. The numbers denote the different *Hin*cII cut sites. (C) 2D-AGE panels from untreated and UV- (2 h), $KBrO_3$- (8 h), and ddC- (48 h) exposed cells. Whereas ddC effectively stalls all types of replication intermediates, UV and treatment results in accumulation of the diffuse RNA:DNA hybrid–containing replication bubbles (db). Autoradiographs represent comparative exposures.

(Figure 7C). Of interest, no similar acute effect on ND2 was observed in the $KBrO_3$-treated cells, for which an increase in both ND2 and ND3 levels appeared 32 h after the removal of the drug (Figure 7B). Because the effects of UV and oxidative damage on the expression of mitochondrial genes differ—despite the similar replication phenotype—it is likely that the effects of damage on mtDNA maintenance and gene expression are not connected.

The fact that we did not observe an increase in transcription preceding the accumulation of RITOLS intermediates fits the idea that they contain processed heavy-strand mRNAs (Reyes *et al.*, 2013). This indicates that RITOLS replication is not dependent on de novo transcription but uses existing RNA molecules. Recruiting and annealing RNA at the replication fork quite likely requires a dedicated enzymatic machinery, so far unprecedented or overlooked in any other genome maintenance system known to exist. In fact, it has also been suggested that RITOLS would be an artifact due to RNA pairing with single-strand DNA in vitro (Miralles Fuste *et al.*, 2014). Although taking into account that cross-linking experiments have demonstrated that RNA:DNA hybrids are present in vivo (Reyes *et al.*, 2013), RITOLS replication should also make sense by having a biologically significant role in mitochondria in order to stand its ground. One such role could relate to the differential mtDNA maintenance strategies required in different tissues. When damaged mtDNA is present, the copy number could be maintained by

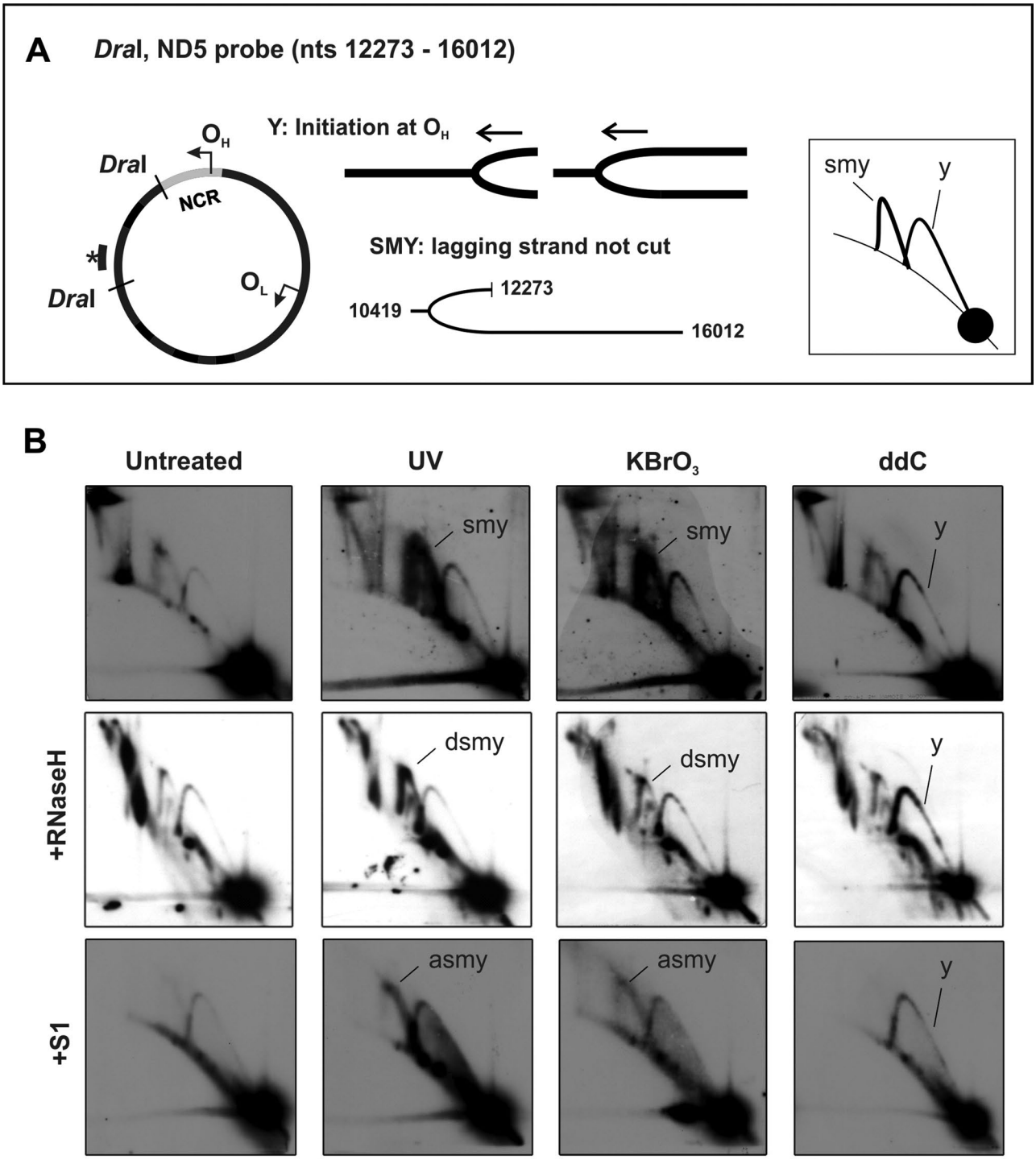


FIGURE 4: UV and $KBrO_3$ treatments specifically increase the levels RNA:DNA hybrid–containing replication intermediates. (A) Diagram of mtDNA, showing the analyzed *DraI* fragment 12,273–16,012 and probe location. Replication initiating at $O_H$ will process to this region unidirectionally, giving rise to only simple (y) and a slow-moving Y-arc (smy). (B) UV and $KBrO_3$ specifically increase the intensity of the smy arc, whereas ddC treatment results in uniform stalling of all replication intermediates. Because the smy arcs contain RNA:DNA hybrids, they are modified by RNaseH, resulting in collapsed degraded smys (dsmy). Of interest, the ascending smy (asmy) in the UV- and $KBrO_3$-treated samples is resistant to single-strand nuclease S1, which normally cleaves RITOLS intermediates effectively. Autoradiographs represent comparative exposures.

increasing replication initiation while maintaining a constant turnover of the most badly damaged templates. In support of this idea, we witnessed a marked increase in replication bubbles outside the conventional $O_H$ origin, indicating an induction of strand-coupled replication from Ori-Z under genotoxic stress (Figure 5). This replication mode change implies that the strand-coupled replication could

represent a damage-tolerant replication mechanism, therefore explaining its preferential usage in tissues with high energy demand (Pohjoismaki and Goffart, 2011). It has been suggested that RITOLS replication evolved to improve mtDNA replication fidelity (Holt and Jacobs, 2014), and this hypothesis is supported by the hierarchy of events in our recovery experiments. Despite some nuances in the details, both UV and $KBrO_3$ treatments seem to first induce an accumulation of RITOLS intermediates, followed by an increase in COSCOFA replication, while maintaining the excess in RITOLS long after the initial insult (Figure 5 and Supplemental Figure S2). In contrast, ddC treatment causes an overall increase in replication intermediates, followed by accumulation of RITOLS in the recovery phase (Figure 6). Our interpretation is that mitochondria adapt to the extensive mtDNA damage first by promoting the damage-tolerant, but perhaps error-prone, COSCOFA mechanism for survival. After the stress is lifted, they revert to RITOLS. The prolonged increase in RITOLS after the recovery could be due to prolonged maturation of these intermediates as the RNA is used as a backup template to contain the mutagenic effects of the damage.

It is curious that the effects of relatively low levels of damage cause such a remarkable change in the mtDNA maintenance and that some of the effects persist for up to 32 h of recovery (Supplemental Figure S4). At least oxidative damage should be quite normal to mitochondria, and the damaged nucleotides should be cleared away by mitochondrial base excision repair after the stress has been lifted. It is tempting to speculate that UV and $KBrO_3$ induce mitohormesis, an adaptive change in mitochondrial retrograde signaling, resulting in better stress tolerance (Yun and Finkel, 2014). Because $H_2O_2$ treatment did not induce a similar modification of replication intermediates, it is likely that ROS alone is not the culprit. Moreover, the similar accumulation of RITOLS intermediates after ddC treatment, a drug specific for mitochondrial polymerase gamma (POLG), also suggests that the effect of UV and $KBrO_3$ would be mtDNA specific and not caused by a bystander effect from the nDNA damage.

Another interesting feature of the UV and $KBrO_3$ treatments, as well as in the recovery from ddC treatment, was the appearance of cruciform molecules (x and xr in Figures 5 and 6). Besides regular x-forms, which are twice the restriction fragment length (2*n*) and likely represent true Holliday junctions, smaller xr-forms also were detected. Because the latter arise furcating from the Y-arc, they could represent regressed replication forks as seen in many other occasions in yeast and prokaryotic chromosomes under replication stress (Cotta-Ramusino *et al.*, 2005; Long and Kreuzer, 2008). Because replication fork regression is an active process, mitochondria must possess an enzymatic machinery to deal with stalled replication forks. Such machinery might have consequences also for the generation of pathological mtDNA rearrangements. Regressed forks themselves can convert to true Holliday junctions, or the x-forms can arise from recombination used to repair the double-strand break caused by the collapsed replication fork (Petermann and Helleday, 2010).

From our study, it can be concluded that UV and $KBrO_3$ can be used to damage mtDNA in an experimental setting, with only a low level of collateral nDNA damage that does not influence host cell survival. The reported effects in mtDNA maintenance are biologically relevant, as the cells tolerate the insult and do not show a significant activation of nuclear stress to a level that persists as long as the effects on mitochondria. Moreover, the outcomes of different stressors are similar, despite the very different types of damage that they induce. For example, compared with the nuclear genome (Kawanishi and Murata, 2006), mtDNA reacts surprisingly strongly to $KBrO_3$. Of interest, $KBrO_3$ has similar ototoxicity as aminoglycoside antibiotics in affecting mitochondrial protein synthesis (Kurokawa *et al.*, 1990; Jacobs, 1997); thus its specificity as a mitochondrial poison should be investigated further. The fate of stalled mtDNA replication forks, as well as the identification of proteins involved in their processing, is likely to hold the key to understanding how pathological mtDNA rearrangements arise. Another and biologically more fundamental challenge will be to find factors involved in governing the preferred replication mode in different tissues. As we demonstrated here, mtDNA replication can be experimentally manipulated, and, perhaps in combination of manipulation of key candidate proteins, it will be possible to interrogate this enigmatic system and make sense of its biology.

## MATERIALS AND METHODS

### Cell culture, ddC, KBrO3 $H_2O_2$ and UV light treatment

HEK293T cells were cultured in DMEM (Biowest, Nuaillé, France) containing 4.5 g/l glucose, 2 mM L-glutamine, 1 mM sodium pyruvate, 50 µg/ml uridine, and 10% fetal bovine serum at 37°C in a humidified atmosphere with 8.5% $CO_2$.

All reagents were from Sigma (Steinheim, Germany) and enzymes from Life Technologies (Carlsbad, CA), except where stated.

To induce oxidative damage, the cells were treated for up to 24 h with 30 µM $KBrO_3$ or 200 µM $H_2O_2$. The relatively low concentration of $KBrO_3$ was chosen to avoid off-target effects in the cells (Kawanishi and Murata, 2006), whereas $H_2O_2$ was used as control for a more generalized oxidative damage (Kuo *et al.*, 2012). An 8-h $KBrO_3$ exposure was chosen for the recovery studies, as it was sufficient to induce oxidation of mtDNA (Figure 1A) but did not yet influence mtDNA topology (Figure 1C). To induce UV damage, the cells were exposed once to 1.34 mJ/cm$^2$, 305-nm wavelength UVB for 30 s using a Benchtop 2UV transilluminator (UVP). No effect on cell growth or proliferation was observed in any of the treatments (Supplemental Figure S1). As control for mitochondrial DNA replication stalling, the cells were treated for 48 h with 175 µM ddC (or zalcitabine), a well-known and highly specific inhibitor of the mtDNA polymerase POLG (Wanrooij *et al.*, 2007). ddC is a nucleotide analogue that is easily incorporated by POLG during mtDNA replication but removed only with very low efficiency, inducing chain termination events and therefore mtDNA replication stalling (Huang *et al.*, 2013). For treatment–recovery experiments, the cells were treated as described, after which the medium was removed, followed by one wash with phosphate-buffered saline and addition of fresh medium without the drug. For experiments lasting >2 d, the medium was replaced every 48 h and cells split so that ~80% confluency was not exceeded.

### Mitochondrial DNA levels and conformation

Total cellular DNA was isolated using proteinase K and SDS lysis, followed by phenol:chloroform extraction and ethanol precipitation (Pohjoismaki *et al.*, 2006). mtDNA copy numbers were analyzed by separating 1 µg of *Bam*HI (cuts human mtDNA once)-digested total DNA on a 0.4% agarose gel in 1× Tris/borate/EDTA (TBE) at 1.2 V/cm for 16 h at room temperature. For mtDNA topology studies, 1 µg of total DNA was digested with *Bgl*II (does not cut mtDNA) following by separation as before. Southern blotting was performed using standard procedures and blots probed for mtDNA with ND5 as mitochondrial probe and 18S rDNA as loading control, using a random primed $^{32}$P-probe spanning nucleotides 12,992–13,670 (ND5) of the human mtDNA or 24–772 (18S rDNA; National Center for Biotechnology Information [NCBI] accession number M10098). The radioactive signal was quantified using phosphor storage imaging (BAS-IP MS screens; GE Healthcare; and Molecular Imager FX; Bio-Rad, Hercules, CA).

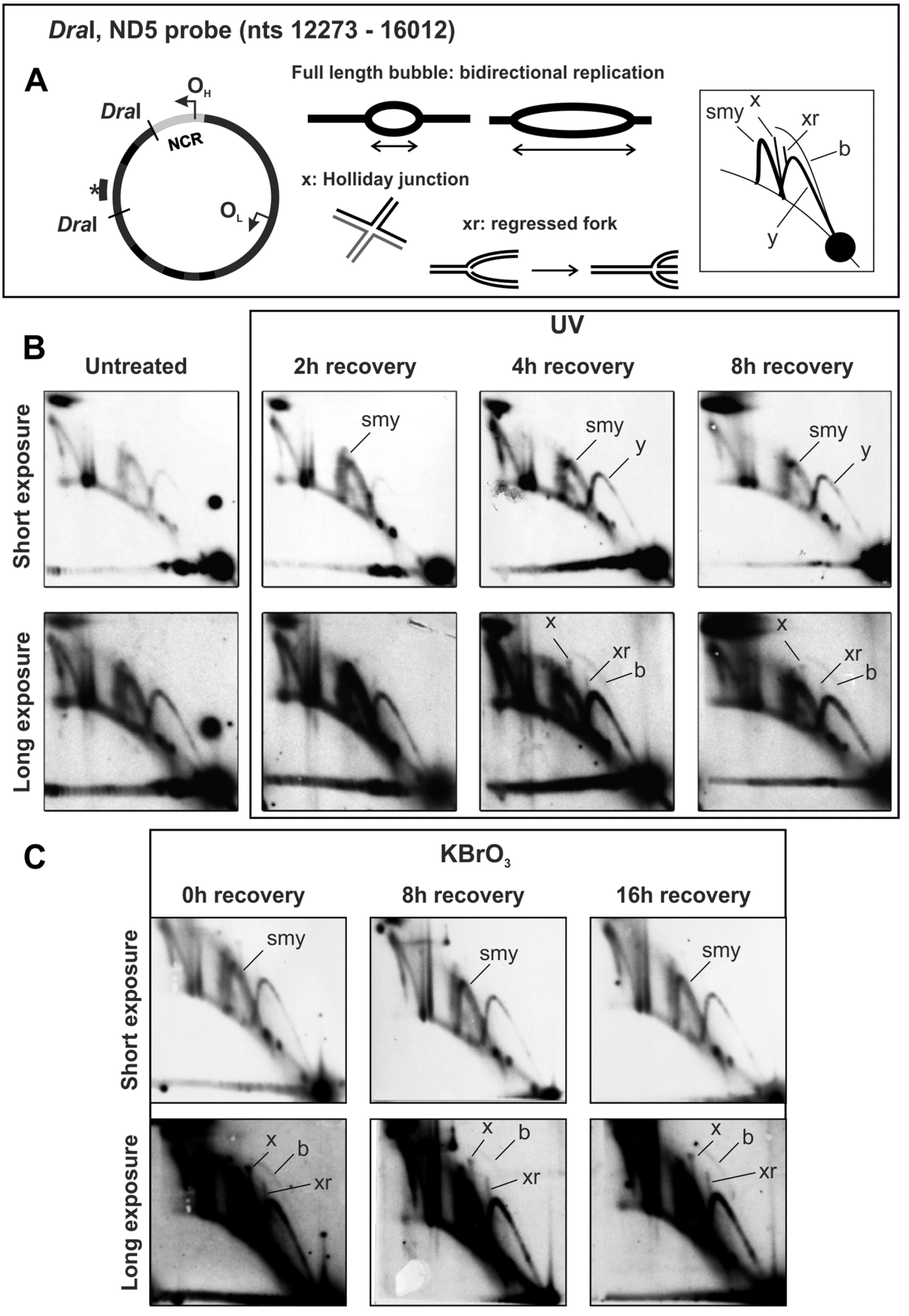
DraI, ND5 probe (nts 12273 - 16012)
A
DraI
NCR
DraI
Full length bubble: bidirectional replication
x: Holliday junction
xr: regressed fork
smy
x
xr
b
y
B
UV
Untreated
2h recovery
4h recovery
8h recovery
Short exposure
Long exposure
C
KBrO3
0h recovery
8h recovery
16h recovery

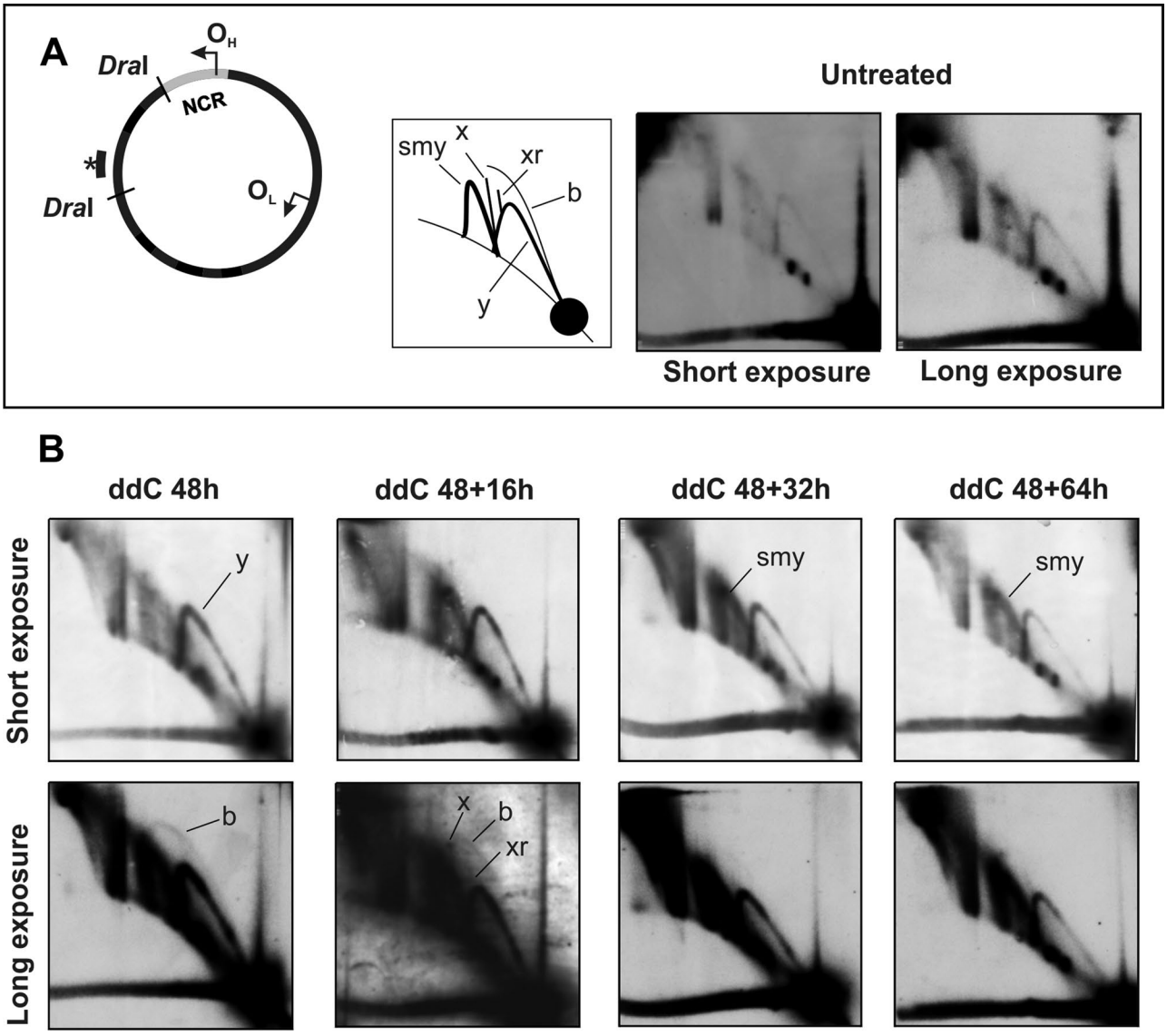


FIGURE 6: The recovery from ddC-induced mtDNA depletion also involves a persisting increase in RITOLS replication. (A) Schematic overview of mtDNA as previously, together with *Dra*I 12,273–16,012 2D-AGE panels of untreated cells, showing the normally occurring forms of replication intermediates. (B) The treatment of cells with ddC results in strong depletion of mtDNA copy number (Supplemental Figure S3) and stalling of all types of replication intermediates. In contrast to the UV and $KBrO_3$ treatment, the recovery from ddC treatment does not involve an increase in x-forms and bubble arcs. However, the relative quantity of smy arcs stays elevated until 64 h, despite the copy number returning to normal levels already after 32 h (Supplemental Figure S3). Autoradiographs represent comparative exposures.

FIGURE 5: The recovery from UV and $KBrO_3$ treatments involves fork regression, Holliday junction formation, and replication initiation outside of NCR. (A) Because *Dra*I 12,273–16,012 lies outside of the NCR, any full-length replication bubbles (b) in the region must represent bidirectional replication initiating at origins (Ori-Z) within the fragment. Four-way junctional molecules can be either true Holliday junctions (x) comprising two restriction fragment–sized molecules (2*n*) or regressed forks (xr), where the free end of the fork has branch migrated and forms a chicken foot–type structure. Whereas true Holliday junctions start from the 2*n* position on the linear arc, the chicken foot is an extension of the y-arc. (B) The smys accumulate quickly after the initial UV exposure, followed by a marked increase in regular y-forms. Longer exposure of the same blot reveals the appearance of x-forms and bubble arcs (b). (C) A similar outcome can be observed in the recovery of cells treated with 30 μM $KBrO_3$ for 8 h before the removal of the drug. It should be noted that, unlike UV, $KBrO_3$ will take some time to wash out from the cells completely. Remarkably, the effect of UV and $KBrO_3$ on RITOLS intermediates will last for up to 64 h (Supplemental Figure S4). Autoradiographs represent comparative exposures.

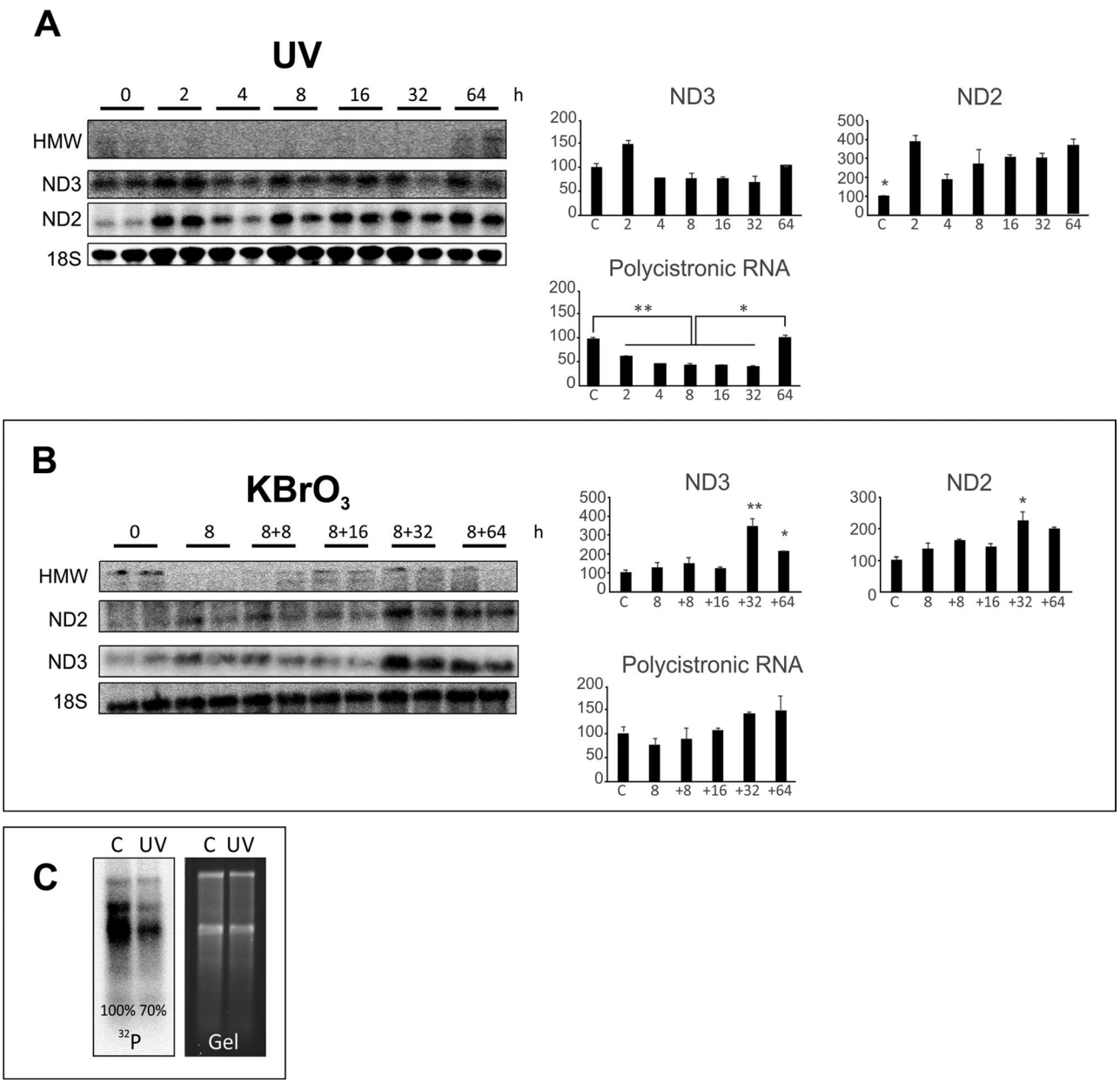


FIGURE 7: UV and $KBrO_3$ affect the steady-state levels of some mitochondrial mRNAs. (A) Cells were treated with UV as before and allowed to recover for 64 h. ND2 mRNA levels show a sharp increase immediately after the treatment. Although the ND3 levels are not affected by UV, the high–molecular weight (HMW) polycistronic RNA detected by the same probe is depleted by the treatment and returns to normal levels only after 32 h. (B) In contrast, in cells exposed to 30 μM $KBrO_3$ for 8 h and allowed to recover for 64 h, both ND2 and ND3 levels increase after 32 h, without a significant effect on the polycistronic RNA. Nuclear 18S is used as a loading control. Results are presented as mean ±SD and *p* values based on one-way analysis of variance with Newman–Keuls test (**$p < 0.01$, *$p < 0.05$). (C) In organello metabolic labeling of mitochondrial transcripts using [$^{32}$P]UTP. UV treatment caused a marked reduction of newly synthesized mitochondrial RNAs (left). Ethidium bromide stain of the same gel is given as the loading control.

**Mitochondrial DNA isolation, 2D-AGE, and Southern blotting**

Mitochondrial DNA was isolated from mitochondria using cytochalasin B treatment before cell breakage, followed by differential and sucrose gradient centrifugation steps as described in Yasukawa *et al.* (2006). The 2D-AGE analysis was performed essentially as described (Pohjoismaki *et al.*, 2006; Wanrooij *et al.*, 2007). Briefly, 5 μg of total mitochondrial nucleic acids was digested with FastDigest *Hin*cII or *Dra*I according to the manufacturer's recommendation and separated over a 0.4% first dimension and a 0.95% second dimension agarose gel in 1× TBE. Southern blotting was performed as described. The blots were probed against nucleotides 12,273–16,012 (*Dra*I) or 13,638–1009 (*Hin*cII) using probes spanning nucleotides 12,992–13,670 (ND5) or 35–611 (NCR) of the human mtDNA.

**mtDNA damage quantification**

Mitochondrial DNA was isolated as described, and 2 μg of total mitochondrial nucleic was spotted onto a nitrocellulose membrane (Amersham Protran; GE Healthcare Life Sciences, Piscataway, NJ)

and as a duplicate on a nylon membrane (Hybond-XL; Amersham, GE Healthcare Life Sciences, Piscataway, NJ) and cross-linked by baking for 2 h at 80°C. The nylon membrane was used to quantify mtDNA by Southern blot as described. The nitrocellulose membrane was used for South-Western detection of 8-oxodG and thymidine dimers: the membranes were blocked in 5% nonfat milk in Tris-buffered saline/Tween-20 overnight and incubated with primary antibody overnight (mouse anti–8-oxodG, 1:250, Ab64548, or mouse anti–thymidine dimers, 1:1000, Ab10347; Abcam, Cambridge, UK). Goat anti-mouse immunoglobulin–horseradish peroxidase (ABIN101744, Antibodies online; Life Technologies, Carlsbad, CA) was used as a secondary antibody at 1:10.000 dilution. The chemiluminescence was quantified using a BioSpectrum 810 imaging System (UVP). To verify both anti–8-oxodG and anti–thymidine dimers antibodies, 2 µg of untreated HEK293 mtDNA was exposed in vitro to 3.1 M $H_2O_2$ for 30 min or 1.34 mJ/cm$^2$ s UVB (305 nm) for 5 min, followed by a South-Western analysis as described.

### Northern blot

RNA for Northern blot was extracted using TRI reagent (Sigma) following the manufacturer's recommendations. A total of 3 µg RNA was separated over a 1.5% agarose 3-(*N*-morpholino)propanesulfonic acid/formaldehyde gel and blotted using standard procedures. Mitochondrial RNA levels were quantified using ND2 (4470–5511) and ND3 (10,131–10,382) probes and 18S rDNA (nucleotides 24–772; NCBI accession number M10098) probe as loading control. The full-length polycistronic RNA was quantified using ND3 hybridization (Koulintchenko *et al.*, 2006).

### Metabolic labeling of RNA in organello

Labeling of mitochondrial RNA in isolated mitochondria was performed as described previously (Reyes *et al.*, 2013). Crude mitochondria from control and UV-treated HEK 293 cells were isolated using cytochalasin B treatment before cell breakage as for mtDNA isolation but followed by differential centrifugation steps instead of the sucrose gradient purification (Yasukawa *et al.*, 2006). The crude mitochondria were washed once in homogenization buffer and equilibrated in incubation buffer (10 mM Tris, pH 8.0, 20 mM sucrose, 20 mM glucose, 75 mM D-sorbitol, 100 mM KCl, 20 mM $K_2HPO_4$, 0,05 mM EDTA, 1 mM ADP, 5 mM $MgCl_2$, 5 mM L-glutamate, 5 mM malate). In organello transcription was performed by incubating the crude mitochondria at 37°C for 30 min in incubation buffer supplemented with all four dNTPs (50 mM each) to prevent any effect on mitochondrial DNA replication; RNA synthesis was supported by addition of ATP, CTP, and GTP (50 mM each). In addition, 34 nM [$^{32}$P]UTP (3000 Ci/mmol; Perkin Elmer-Cetus, Waltham, MA) was used for the metabolic labeling of newly synthesized RNA. After the incubation mitochondria were recovered by sucrose gradient centrifugation as previously described for the 2D-AGE, mitochondrial RNA was isolated from the purified mitochondria using the InnoPREP RNA Mini Kit (Analytik Jena, Biometra, Jena, Germany) and analyzed by Northern blot as described. The gel was run in the presence of 500 ng/ml ethidium bromide to monitor the loading, dried for 2 h at 80°C, and exposed on a phosphoimager screen to quantify the incorporated radioactivity.

## ACKNOWLEDGMENTS

We thank Riitta Pietarinen and Nina Kekäläinen for technical support. This study was supported by the Jane and Aatos Erkko Foundation (J.P.) and the Finnish Academy (S.G.). Funding for the open access charge was from the Jane and Aatos Erkko Foundation.

## REFERENCES

Aller P, Rould MA, Hogg M, Wallace SS, Doublie S (2007). A structural rationale for stalling of a replicative DNA polymerase at the most common oxidative thymine lesion, thymine glycol. Proc Natl Acad Sci USA 104, 814–818.

Ballmaier D, Epe B (1995). Oxidative DNA damage induced by potassium bromate under cell-free conditions and in mammalian cells. Carcinogenesis 16, 335–342.

Bendich AJ (2013). DNA abandonment and the mechanisms of uniparental inheritance of mitochondria and chloroplasts. Chromosome Res 21, 287–296.

Bowmaker M, Yang MY, Yasukawa T, Reyes A, Jacobs HT, Huberman JA, Holt IJ (2003). Mammalian mitochondrial DNA replicates bidirectionally from an initiation zone. J Biol Chem 278, 50961–50969.

Cheng KC, Cahill DS, Kasai H, Nishimura S, Loeb LA (1992). 8-Hydroxyguanine, an abundant form of oxidative DNA damage, causes G→T and A→C substitutions. J Biol Chem 267, 166–172.

Cotta-Ramusino C, Fachinetti D, Lucca C, Doksani Y, Lopes M, Sogo J, Foiani M (2005). Exo1 processes stalled replication forks and counteracts fork reversal in checkpoint-defective cells. Mol Cell 17, 153–159.

Floyd RA, Watson JJ, Wong PK, Altmiller DH, Rickard RC (1986). Hydroxyl free radical adduct of deoxyguanosine: sensitive detection and mechanisms of formation. Free Radical Res Commun 1, 163–172.

Frenkel K, Goldstein MS, Teebor GW (1981). Identification of the cis-thymine glycol moiety in chemically oxidized and gamma-irradiated deoxyribonucleic acid by high-pressure liquid chromatography analysis. Biochemistry 20, 7566–7571.

Goffart S, Cooper HM, Tyynismaa H, Wanrooij S, Suomalainen A, Spelbrink JN (2009). Twinkle mutations associated with autosomal dominant progressive external ophthalmoplegia lead to impaired helicase function and in vivo mtDNA replication stalling. Hum Mol Genet 18, 328–340.

Greaves LC, Reeve AK, Taylor RW, Turnbull DM (2012). Mitochondrial DNA and disease. J Pathol 226, 274–286.

Gredilla R, Bohr VA, Stevnsner T (2010). Mitochondrial DNA repair and association with aging—an update. Exp Gerontol 45, 478–488.

Han M, Im DS (2008). Effects of mitochondrial inhibitors on cell viability in U937 monocytes under glucose deprivation. Arch Pharm Res 31, 749–757.

Holt IJ, Jacobs HT (2014). Unique features of DNA replication in mitochondria: a functional and evolutionary perspective. BioEssays 36, 1024–1031.

Holt IJ, Reyes A (2012). Human mitochondrial DNA replication. Cold Spring Harb Perspect Biol 4, a012971.

Huang SY, Murai J, Dalla Rosa I, Dexheimer TS, Naumova A, Gmeiner WH, Pommier Y (2013). TDP1 repairs nuclear and mitochondrial DNA damage induced by chain-terminating anticancer and antiviral nucleoside analogs. Nucleic Acids Res 41, 7793–7803.

Jacobs HT (1997). Mitochondrial deafness. Ann Med 29, 483–491.

Kaniak-Golik A, Skoneczna A (2015). Mitochondria-nucleus network for genome stability. Free Radic Biol Med 82, 73–104.

Kawanishi S, Murata M (2006). Mechanism of DNA damage induced by bromate differs from general types of oxidative stress. Toxicology 221, 172–178.

Koulintchenko M, Temperley RJ, Mason PA, Dietrich A, Lightowlers RN (2006). Natural competence of mammalian mitochondria allows the molecular investigation of mitochondrial gene expression. Hum Mol Genet 15, 143–154.

Krishnan KJ, Reeve AK, Samuels DC, Chinnery PF, Blackwood JK, Taylor RW, Wanrooij S, Spelbrink JN, Lightowlers RN, Turnbull DM (2008). What causes mitochondrial DNA deletions in human cells? Nat Genet 40, 275–279.

Kuo ML, Sy AJ, Xue L, Chi M, Lee MT, Yen T, Chiang MI, Chang L, Chu P, Yen Y (2012). RRM2B suppresses activation of the oxidative stress pathway and is up-regulated by p53 during senescence. Sci Rep 2, 822.

Kurokawa Y, Maekawa A, Takahashi M, Hayashi Y (1990). Toxicity and carcinogenicity of potassium bromate–a new renal carcinogen. Environ Health Perspect 87, 309–335.

Lagouge M, Larsson NG (2013). The role of mitochondrial DNA mutations and free radicals in disease and ageing. J Intern Med 273, 529–543.

Liu P, Demple B (2010). DNA repair in mammalian mitochondria: much more than we thought? Environ Mol Mutagen 51, 417–426.

Long DT, Kreuzer KN (2008). Regression supports two mechanisms of fork processing in phage T4. Proc Natl Acad Sci USA 105, 6852–6857.

McCulloch SD, Kokoska RJ, Chilkova O, Welch CM, Johansson E, Burgers PM, Kunkel TA (2004). Enzymatic switching for efficient and accurate translesion DNA replication. Nucleic Acids Res 32, 4665–4675.

Miralles Fuste J, Shi Y, Wanrooij S, Zhu X, Jemt E, Persson O, Sabouri N, Gustafsson CM, Falkenberg M (2014). In vivo occupancy of mitochondrial single-stranded DNA binding protein supports the strand displacement mode of DNA replication. PLoS Genet 10, e1004832.
Petermann E, Helleday T (2010). Pathways of mammalian replication fork restart. Nat Rev Mol Cell Biol 11, 683–687.
Peterson CL, Almouzni G (2013). Nucleosome dynamics as modular systems that integrate DNA damage and repair. Cold Spring Harb Perspect Biol 5, a012658.
Pinto M, Moraes CT (2014). Mitochondrial genome changes and neurodegenerative diseases. Biochim Biophys Acta 1842, 1198–1207.
Pohjoismaki JL, Boettger T, Liu Z, Goffart S, Szibor M, Braun T (2012). Oxidative stress during mitochondrial biogenesis compromises mtDNA integrity in growing hearts and induces a global DNA repair response. Nucleic Acids Res 40, 6595–6607.
Pohjoismaki JL, Goffart S (2011). Of circles, forks and humanity: topological organisation and replication of mammalian mitochondrial DNA. BioEssays Biol 33, 290–299.
Pohjoismaki JL, Goffart S, Spelbrink JN (2011). Replication stalling by catalytically impaired Twinkle induces mitochondrial DNA rearrangements in cultured cells. Mitochondrion 11, 630–634.
Pohjoismaki JL, Goffart S, Tyynismaa H, Willcox S, Ide T, Kang D, Suomalainen A, Karhunen PJ, Griffith JD, Holt IJ, Jacobs HT (2009). Human heart mitochondrial DNA is organized in complex catenated networks containing abundant four-way junctions and replication forks. J Biol Chem 284, 21446–21457.
Pohjoismaki JL, Wanrooij S, Hyvarinen AK, Goffart S, Holt IJ, Spelbrink JN, Jacobs HT (2006). Alterations to the expression level of mitochondrial transcription factor A, TFAM, modify the mode of mitochondrial DNA replication in cultured human cells. Nucleic Acids Res 34, 5815–5828.
Pohjoismaki JL, Williams SL, Boettger T, Goffart S, Kim J, Suomalainen A, Moraes CT, Braun T (2013). Overexpression of Twinkle-helicase protects cardiomyocytes from genotoxic stress caused by reactive oxygen species. Proc Natl Acad Sci USA 110, 19408–19413.
Reyes A, Kazak L, Wood SR, Yasukawa T, Jacobs HT, Holt IJ (2013). Mitochondrial DNA replication proceeds via a "bootlace" mechanism involving the incorporation of processed transcripts. Nucleic Acids Res 41, 5837–5850.
Spiegelman BM (2007). Transcriptional control of energy homeostasis through the PGC1 coactivators. Novartis Found Symp 286, 3–6; discussion 6–12, 162–163, 196–203.
Wagner BA, Witmer JR, van 't Erve TJ, Buettner GR (2013). An assay for the rate of removal of extracellular hydrogen peroxide by cells. Redox Biol 1, 210–217.
Wanrooij S, Goffart S, Pohjoismaki JL, Yasukawa T, Spelbrink JN (2007). Expression of catalytic mutants of the mtDNA helicase Twinkle and polymerase POLG causes distinct replication stalling phenotypes. Nucleic Acids Res 35, 3238–3251.
Yasukawa T, Reyes A, Cluett TJ, Yang MY, Bowmaker M, Jacobs HT, Holt IJ (2006). Replication of vertebrate mitochondrial DNA entails transient ribonucleotide incorporation throughout the lagging strand. EMBO J 25, 5358–5371.
Yeeles JT, Marians KJ (2011). The Escherichia coli replisome is inherently DNA damage tolerant. Science 334, 235–238.
Yun J, Finkel T (2014). Mitohormesis. Cell Metab 19, 757–766.